Int. J. Multiphase Flow, Vol. 2, pp. 247–259. Pergamon/Elsevier, 1975. Printed in Great Britain.

TURBULENCE STRUCTURE OF AIR–WATER BUBBLY FLOW—III. TRANSPORT PROPERTIES

AKIMI SERIZAWA
Institute of Atomic Energy, Kyoto University, Uji, Kyoto, Japan

and

ISAO KATAOKA and ITARU MICHIYOSHI
Department of Nuclear Engineering, Kyoto University, Sakyo-ku, Kyoto, Japan

(*Received* 1 *September* 1974)

Abstract—An experimental study of heat and bubble transport in turbulent air–water bubbly flow was carried out by means of tracer techniques. Helium tracer gas concentration data and temperature distributions were used to extract bubble and heat diffusivity information. The results indicated that the turbulent velocity components of the liquid phase play a predominant role in the turbulent transport process. A systematic increase of diffusivity of heat, ϵ_H, with quality and water velocity was observed. An empirical correlation for the diffusivity ratio $\epsilon_{H,TP}/\epsilon_{H,SP}$ is presented. The Péclet number, $u'_c\bar{d}/\phi$, for bubble dispersion can be approximated by 2.0, independent of the flow variables. The bubble-to-heat diffusivity ratio, ϕ/ϵ_H, approaches unity with increasing quality and water velocity. Momentum transport is also discussed, based on a mixing length theory.

INTRODUCTION

As shown in the preceeding paper in this series, the distributions of transferable quantities such as the void fraction and the velocities of the two phases are very sensitive to the turbulent transport process, which is dependent entirely on both random fluid motion and random bubble motions. The degree of uniformity of distribution of those quantities is severely dependent on the competition between the inertial force and random mixing actions of the liquid, caused mainly by random bubble motions. It is the mechanism of the turbulence and of its transport process governing the two-phase bubbly flow that we want to consider in detail.

In previous turbulence investigations, measurements of the eddy diffusivity of momentum, mass, and heat have been intended for the structural analysis of single-phase flow (Hinze 1959). However, many attempts have recently been carried out in order to get an indication of particle diffusivity in gas–solid systems (e.g. Hino 1967; Briller & Robinson 1969; Suneja & Wasan 1972; Goldschmidt *et al.* 1972), and gas–liquid droplet systems (Cousins & Hewitt 1968; Ginsberg 1971). Knowledge is still lacking for gas bubble–liquid systems (Reith *et al.* 1968; Serizawa *et al.* 1973). Possible turbulent transport rates considered here are the eddy diffusivities for momentum transport, mass (bubble) transport, and heat transport. The eddy diffusivity for bubble transport or the turbulent dispersion coefficient of bubbles is based upon the assumption of the diffusive nature of bubbles and the statistical property of random bubble motions. It also depends upon the assumption of sufficiently small bubble size relative to the smallest turbulence scale.

To clarify the turbulence transport mechanisms in terms of the functions of the turbulent flow field, experiments were conducted to determine the eddy diffusivity of heat and the turbulent dispersion coefficient of bubbles in the central core region of both single-phase water flow and air–water two-phase bubbly flow. Last, we discuss briefly the applicability of a mixing length concept to the present case, and also consider the mechanism of momentum transport in air–water two-phase bubbly flow. The water loop used for the present purpose and the calculating procedures of the diffusivities have been described in the previous papers in this series.

EDDY DIFFUSIVITY OF HEAT

The radial eddy diffusivity of heat was obtained by measuring radial temperature distributions at five axial positions downstream of a line heat source located along the pipe diameter.

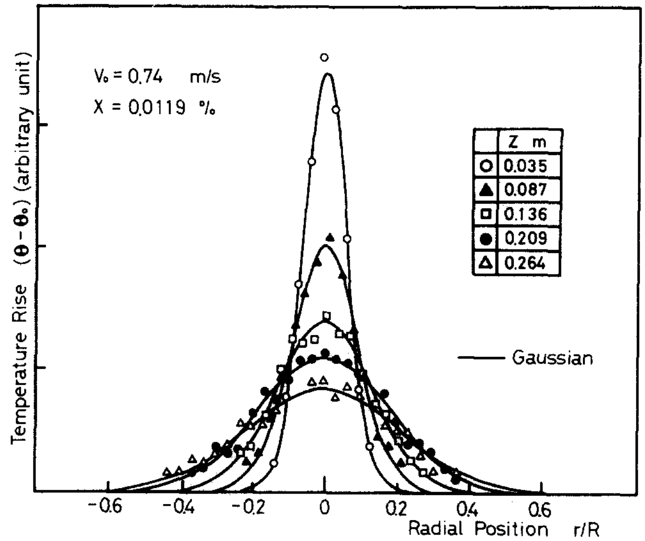

Figure 1. Typical temperature rise profiles.

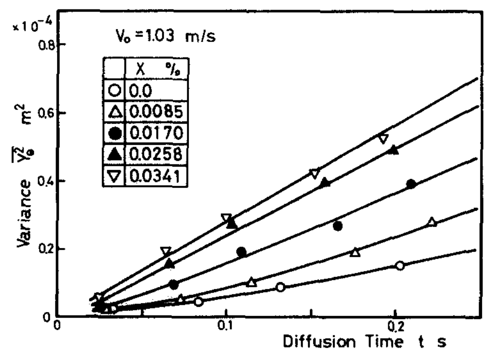

Figure 2. Displacement variance vs diffusion time for heat.

Experimental procedures and the relating technique have been already mentioned in the first paper of this series.†

Typical experimental results appear in figures 1 and 2 showing respectively, the fluid temperature distributions and plots of the variance $\overline{y_\theta(t)^2}$ vs diffusion time t. The data reduction from the profiles to the desired eddy diffusivity ϵ_H is a straight-forward process. The plot of the displacement variance $\overline{y_\theta^2}$ vs diffusion time t shows the following functional dependence (Hinze 1959):

$$\overline{y_\theta(t)^2} = 2\epsilon_H t^*[t/t^* - \{1 - \exp(-t/t^*)\}], \qquad [1]$$

where t^* is the intersection of the asymptote to the curve with the t-axis (for constant velocity, $z = \bar{V}t \propto t$). A least squares procedure was used to fit the calculated variance $\overline{y_\theta^2}$ to [1] and to obtain the eddy diffusivity for heat transport ϵ_H. Results thus obtained are given in figure 3, showing the diffusivity as a function of the quality for constant water velocities. From this figure, it is seen that the diffusivity, varying in the range of $0.2 \sim 1.5 \times 10^{-4}$ m²/sec, increases considerably with quality and also with water flow rate. This trend roughly agrees qualitatively with that observed in turbulent intensity as already shown in the previous paper.

†An analysis of the power spectral density of temperature fluctuation of the mixture suggests that the thermal equilibrium condition between the two phases can be applied to the present situation. Any small heat capacity of bubbles is expected to make much less contributions to the turbulent transport of heat than the liquid.

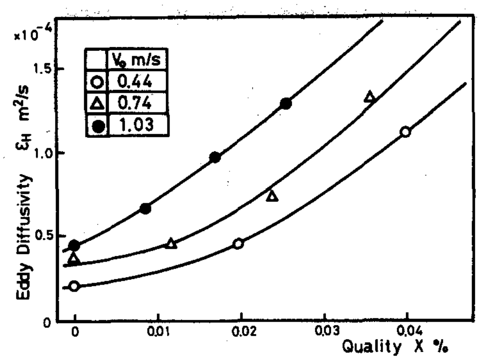

Figure 3. Variation of eddy diffusivity of heat.

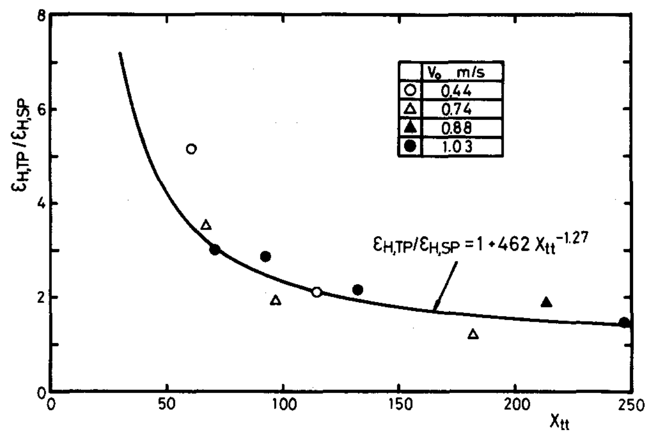

Figure 4. Plots of $\epsilon_{H,TP}/\epsilon_{H,SP}$ vs X_{tt}.

Figure 4 shows a plot of $\epsilon_{H,TP}/\epsilon_{H,SP}$, the ratio of the eddy diffusivity of heat for two-phase flow $\epsilon_{H,TP}$ to that for single-phase water flow $\epsilon_{H,SP}$, in terms of the modulus X_{tt} given by

$$X_{tt} = (1 - X/X)^{0.9}(\rho_g/\rho_l)^{0.5}(\mu_l/\mu_g)^{0.1}. \quad [2]$$

It is seen that the ratio $\epsilon_{H,TP}/\epsilon_{H,SP}$ can be grossly correlated by the following empirical equation, though some data scatter around it and the data shown in the figure were obtained under rather limited range of conditions.

$$\epsilon_{H,TP}/\epsilon_{H,SP} = 1 + 462 X_{tt}^{-1.27}. \quad [3]$$

BUBBLE DISPERSION IN WATER

A study of gas bubble transport in water was carried out both in stationary water in a pool and in turbulent pipe flow. These experiments were preliminary steps to two-phase flow experiments. In the stationary water experiment, air or argon bubbles were introduced, whereas in the flow experiment, primarily argon bubbles. Experimental procedures were common to both cases in many points. As shown in figure 5, the bubbles generated from a point source by means of nozzle atomization were introduced into the water stream and were carried downstream, spreading towards the pipe wall (the bubble injector is a 0.88-mm i.d. stainless steel tube located at the pipe center). In the stationary water experiment a glass basin 300 × 260 × 200 mm in size was used. For various superficial water velocities and volumetric gas flow rates the lateral distributions of bubble impaction rate and local mean bubble velocity were measured by a resistivity probe method at several axial positions downstream of the bubble injector. A water box was used to take photographs of bubbles for bubble radius measurement eliminating the lens effect due to pipe

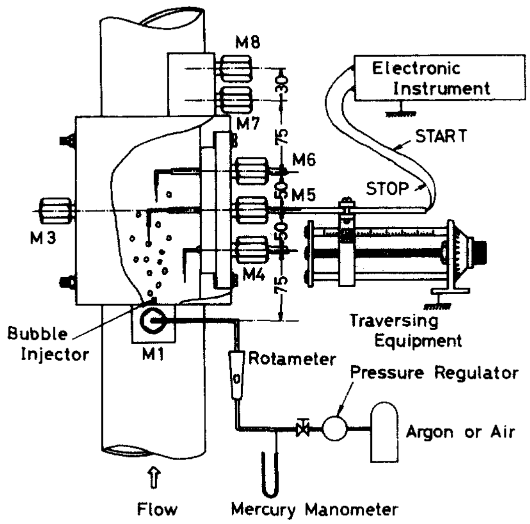

Fig. 5. Details of experimental arrangement.

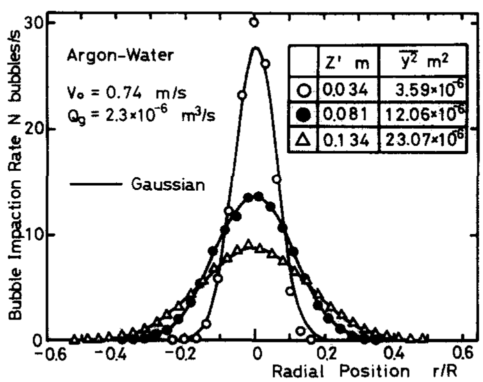

Fig. 6. Typical bubble impaction rate profiles in water.

curvature. In these experiments, the bubble dispersion coefficient was deduced from bubble impaction rate distributions instead of mass concentration distributions according to [14] and [15] in the first paper of this series.

Typical distributions of bubble impaction rate are represented in figure 6, and mean bubble diameter in figure 7. (Most bubbles were oblate spheroidal, of which the a/b ratios were between 1.1 and 1.9, where a and b are the semimajor and the semiminor axes of a spheroidal bubble.) Thus, the lateral distribution of bubble impaction rate can be well represented by a Gaussian distribution (solid lines in figure 6). This means a satisfactory agreement between the bubble diffusion model (e.g. equation[13] in the first paper) and the experimental results. However, it was visually observed that for small dispersion times, bubbles generated at the injector ascended in a bubble-column along a zig-zag path or in a uniform spiral over a certain small distance, and at this stage, bubbles scarcely dispersed laterally into the water†. Figure 8 represents the bubble dispersion coefficient ϕ at large dispersion times as functions of the volumetric gas flow rate Q_g and water velocity V_0. In stationary cases, a rapid increase of ϕ in the range $Q_g \gtrsim 8 \times 10^{-6}$ m^3/sec may result from a change in bubble shape from spheroidal to mushroom with spherical cap and a resultant violent circulation of bulk water, while that observed in the range $Q_g \lesssim 3 \times 10^{-6}$ m^3/sec

†It was shown theoretically by one of the authors (Serizawa 1974) that the assumptions of radially-uniform bubble velocity profile, negligibly small axial diffusion of bubbles, and radially-uniform bubble dispersion coefficient are all valid. It was also shown that the effect of the initial condition for bubble generation is negligibly small for downstream distance from the injector more than about 0.03 m.

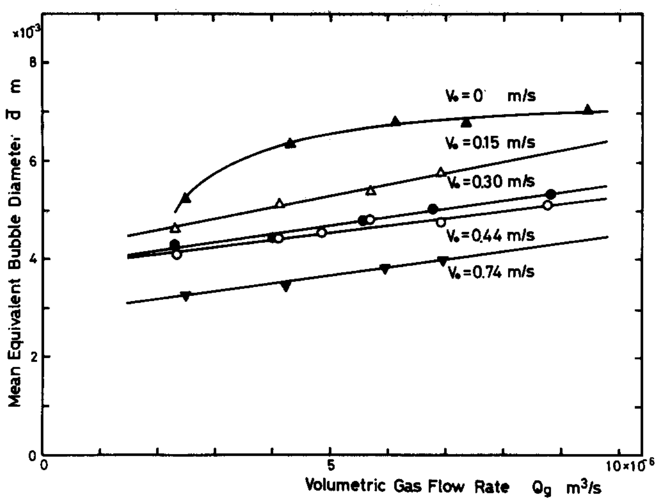

Figure 7. Mean bubble diameter vs volumetric gas flow rate.

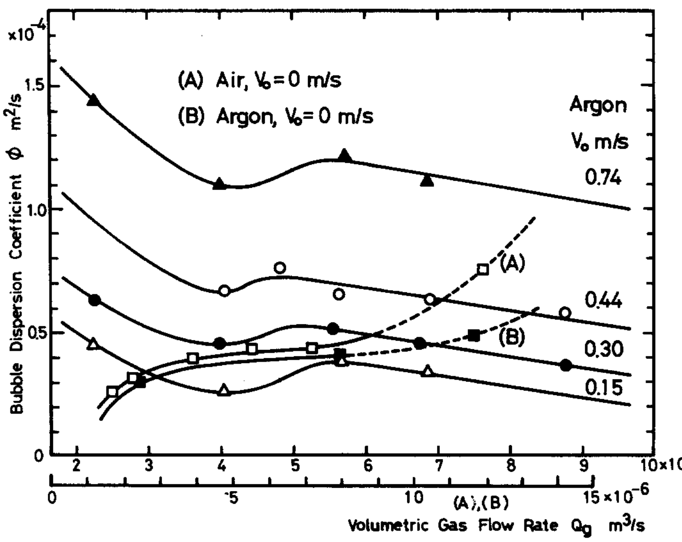

Figure 8. Variation of bubble dispersion coefficient in single-phase water flow.

may be due to a rapid increase in bubble size (figure 7). In the flow experiment, the bubble dispersion coefficient is of the order $0.2 \sim 1.5 \times 10^{-4}$ m²/sec, varying dependently upon the water velocity and gas flow rate. Okamoto *et al.* (1971) reported that the radial number distribution of hydrogen bubbles of about 0.05 mm diameter generated by electrolysis of water was characterized also by Gaussian curve in turbulent water flow. They got 0.52 and 0.47×10^{-4} m²/sec for ϕ at $V_0 = 1.15$ and 0.73 m/sec, respectively, assuming a radially-uniform dispersion coefficient. These values are consistent with our experimental results.

The effect of increasing water velocity is to increase significantly the bubble dispersion coefficient. In consideration of the experimental fact that the turbulent velocity $u'(=\sqrt{\overline{u^2}})$ for $V_0 = 0.74$ m/sec is nearly 1.8 times larger than that for $V_0 = 0.44$ m/sec, whereas in figure 8 the ratio $[\phi]_{V_0=0.74}/[\phi]_{V_0=0.44}$ lies between 1.5 and 2, it will be recognized that the bubble dispersion coefficient is closely related to the turbulent characteristics of the water flow. Figures 7 and 8 indicate more active bubble migration for small bubbles. The effect of gas flow rate upon ϕ can be manifested by more direct effects of bubble size and bubble density.

Experimental evidence suggests two mechanisms for bubble transport process in water: one due to the intrinsic periodic zig-zag or spiral motions of bubbles, and the other due to flow turbulence or agitated liquid characteristics. Namely:

(1) For very small Q_g: zig-zag or spiral motions are predominant.

(2) For (approx. $2\times10^{-6}\leqslant)Q_g\leqslant5\times10^{-6}$ m^3/sec: zig-zag or spiral motions and relatively small flow turbulence or random walks of bubbles are coexistent.

(3) For $Q_g\geqslant5\times10^{-6}$ m^3/sec: bubble diffusion process predominant region where the flow turbulence or random walks of bubbles prevail.

In general, a higher bubble density or higher flow turbulence or heterogeneity of the flow field may suppress periodic zig-zag or spiral motions of bubbles, and may accelerate their random motions. This random walk or random characteristics of bubbles is the nature of bubble diffusivity itself.

BUBBLE DISPERSION IN AIR-WATER TWO-PHASE BUBBLY FLOW

One of the most predominant parameters relating to the turbulence structure of two-phase bubbly flow is the behavior of gas bubbles moving in turbulent flow field. Houghton (1961, 1962) applied a statistical concept to the bubble motion in heated channels in order to estimate the cross-sectional average void fraction profile and bulk temperature profile in the flow direction. Based on the modern theory of the Brownian motion of a free particle, in this case a bubble, he obtained fundamental flux vectors for the diffusion of bubbles in heated channels by considering bubble motion in a turbulent liquid as a Markov process. The analysis by Houghton is quite interesting, but he does not discuss the legitimacy of applying such a bubble diffusion model to the bubble movements in two-phase flow systems. The experimental results shown in the preceding section of this paper suggest that the assumption of random bubble motions, hence a bubble diffusion model, is possibly valid also for air–water two-phase bubbly flow.

The radial turbulent dispersion coefficient of gas bubbles in air–water bubbly flow was obtained by measuring radial concentration distributions of the tracer gas (helium) by means of an isokinetic sampling probe and a gas-chromatograph, assuming that all the hydrodynamic characteristics of helium bubbles, including the diffusivity are equal to the corresponding characteristics of air bubbles. This assumption appears to be correct if we consider the balance of forces acting on a bubble suspended in turbulent flow field (Serizawa 1974). Curves (A) and (B) in figure 8 support this. Detailed descriptions of measurement of the turbulent dispersion of bubbles by means of an isokinetic probe appear in the first paper of this series.

Prior to measurements, dependence of the tracer bubble diffusivity upon its flow rate was examined at three volumetric flow rates of helium, 2.0, 3.5 and 7.7×10^{-6} m^3/sec. The result indicated no significant dependence upon this variable, and the flow rate of helium was set at 7.7×10^{-6} m^3/sec in all runs.

Figures 9 and 10 represent typical experimental results showing, respectively, the mass concentration distributions of helium per unit volume of air–water mixture, and plots of the variance $\overline{y^2}$ against dispersion time t.

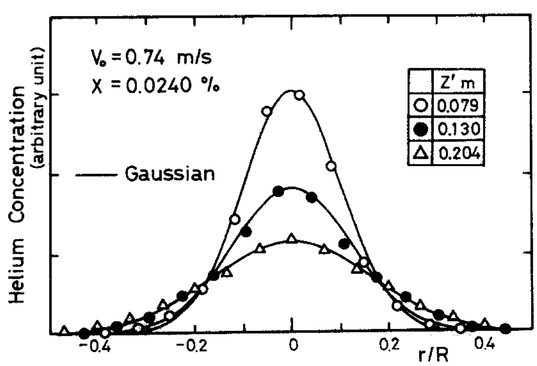

Figure 9. Mass concentration distribution of helium tracer bubbles.

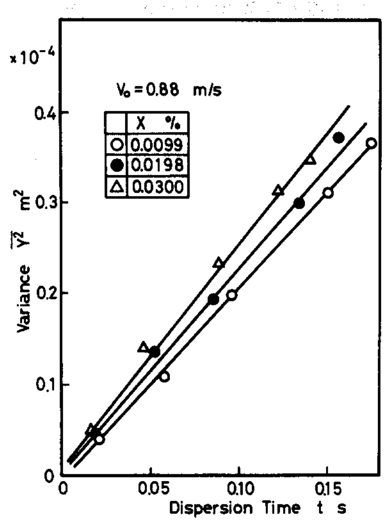

Fig. 10. Displacement variance vs dispersion time.

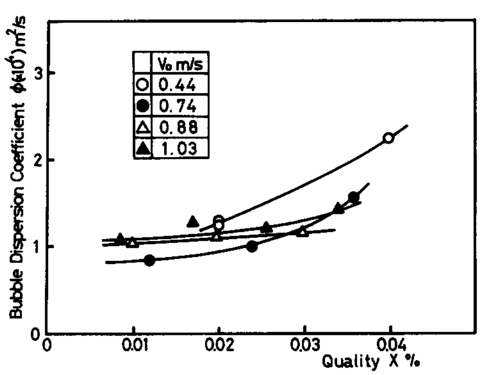

Figure 11. Variation of bubble dispersion coefficient in bubbly flow.

The turbulent dispersion coefficient of bubbles at large dispersion time ϕ deduced from the plots of displacement variance is presented in figure 11 as a function of the quality X and the water velocity. It is seen that the bubble dispersion coefficient increases considerably with an increase in quality for low water velocities, while it increases only slightly for higher water velocities; however it depends only very slightly upon the water velocity. It is notable that in some cases of small quality, ϕ is smaller in bubbly flow than in single-phase water flow. In single-phase water flow, bubble diffusivity is increased mainly by the turbulent velocity components of the water flow which normally increase monotonically with increasing water velocity. In two-phase flow, when the gas flow rate is increased, bubble diffusivity will be determined by the competition among the increased interactions between bubbles, the more effective inertial force of the water accelerated by bubbles, and the resultant increased turbulent velocity components of the water flow. Recalling the experimental fact that in some cases of higher water velocity and small quality the turbulent intensity of the liquid exhibits a lower value than in single-phase water flow (figure 12 in the second paper of this series), we notice a good agreement in dependence upon the quality and the water velocity between those of the turbulent velocity $\sqrt{\overline{u^2}}$ and those for the turbulent dispersion coefficient of bubbles ϕ.

Figure 12 shows a representation of $u'_c\bar{d}/\theta$, the so-called Péclet number, (where $u'_c = \sqrt{\overline{u^2}}$ is the turbulent velocity of the flow field at the pipe center, and $\bar{d}$ is the mean bubble diameter) against the local void fraction at the pipe center α_c. The Péclet number can be set approximately equal to 2.0 independently of the void fraction, despite some scatter of the data. A more detailed inspection of the data reveals a weak dependence of the Péclet number upon void fraction, if the

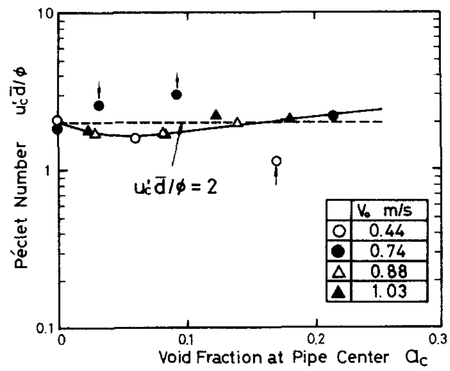

Figure 12. Péclet number vs void fraction at the pipe center.

points with a mark ↓ in the figure are ignored. This results in the conclusion that the direct major mechanism of bubble dispersion both in single-phase water flow and in two-phase bubbly flow is the turbulent transport properties of the liquid phase, and that the interactions between bubbles and the inertial effects are additional mechanisms. It also implies that the effects of the bubble-interaction upon the diffusivity may be suppressed relatively by the inertial effects for higher water velocities. Of course a small gradient of the water velocity with respect to the radius for a higher water velocity and a small quality (figure 11 in the previous paper of this series) may also serve to reduce the lateral spread of bubbles due to the Magnus effect.

Figure 13 represents the ratio ϕ/ϵ_H between the diffusivity for bubble transport and that for heat transport in terms of the quality and the water velocity. This figure presents a trend for the ratio ϕ/ϵ_H to approach unity as the quality and the water velocity become larger, though it strongly depends upon the water velocity. $\phi/\epsilon_H = 1$ means the same mechanism for both the turbulent transport of heat and for bubble transport. Consequently, it is confirmed that the predominant mechanism of bubble transport in an air–water mixture is the turbulent motions of the liquid phase, especially for higher water velocity and higher quality region, since the turbulent diffusivity of heat is determined primarily by the turbulent properties of the liquid phase.

MOMENTUM TRANSPORT PREDICTED BY MIXING LENGTH THEORY

Assuming that the bubbles are sufficiently small with respect to the smallest turbulence scale, the mixing length concept analogous to that proposed by Levy (1963) which considers a homogeneous flow with radial variation of the fluid density will serve to study the transport process in two-phase bubbly flow.

Starting from the equation of motion for steady state, homogeneous, and incompressible two-phase flow with local density

$$\rho = \rho_l(1-\alpha_{loc}) + \rho_g\alpha_{loc} = \rho_l\alpha_l + \rho_g\alpha_{loc}, \qquad [4]$$

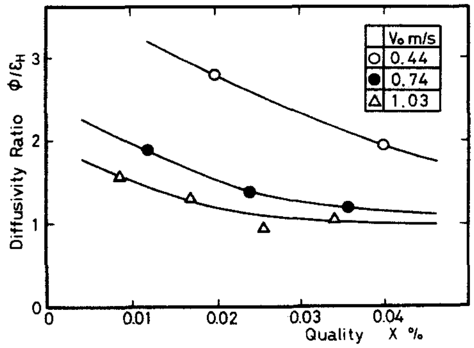

Figure 13. Diffusivity ratio ϕ/ϵ_H vs quality.

where $\alpha_l = 1 - \alpha_{loc}$, Levy's equation becomes with addition of viscous effects†,

$$\tau = \bar{\rho}\overline{uv} + \bar{V}_l\overline{\rho' v} + \mu_l\bar{\alpha}_l(\mathrm{d}\bar{V}_l/\mathrm{d}y), \quad [5]$$

where a bar denotes a time-average.

From an accepted mixing length theory, the turbulent velocity components and fluctuating component of density are

$$u = v = L_v(\mathrm{d}\bar{V}_l/\mathrm{d}y),\ \rho' = L_d(\mathrm{d}\bar{\rho}/\mathrm{d}y). \quad [6]$$

By substituting [6] into [5] and assuming $L_v = L_d = L_m$, we obtain

$$\tau = L_m^2(\mathrm{d}\bar{V}_l/\mathrm{d}y)|\mathrm{d}(\bar{\rho}\bar{V}_l)/\mathrm{d}y| + \mu_l\bar{\alpha}_l(\mathrm{d}\bar{V}_l/\mathrm{d}y)$$

$$\simeq \rho_l L_m^2(\mathrm{d}\bar{V}_l/\mathrm{d}y)|\mathrm{d}(\bar{\alpha}_l\bar{V}_l)/\mathrm{d}y| + \mu_l\bar{\alpha}_l(\mathrm{d}\bar{V}_l/\mathrm{d}y). \quad [7]$$

Hence,

$$L_m = [\{\tau - \mu_l\bar{\alpha}_l(\mathrm{d}\bar{V}_l/\mathrm{d}y)\}/\rho_l(\mathrm{d}\bar{V}_l/\mathrm{d}y)|\mathrm{d}(\bar{\alpha}_l\bar{V}_l)/\mathrm{d}y|]^{1/2}. \quad [8]$$

Local shear stress $\tau(r)$ can be determined by the force balance as

$$\tau(r) = -\frac{1}{r}\int_0^r [\bar{\rho}g + (\mathrm{d}\bar{P}/\mathrm{d}z)_t]r\,\mathrm{d}r, \quad [9]$$

where $(\mathrm{d}\bar{P}/\mathrm{d}z)_t$ is total pressure drop. Combination of [8] and [9] makes it possible to calculate the mixing length for momentum transport from the measured distributions of the phases and the water velocity (Aoki *et al.* 1969). The mixing length for velocity can be also deduced from the experimental data of the liquid velocity and the corresponding turbulent intensity:

$$L_v = \sqrt{\overline{u^2}}/|\mathrm{d}\bar{V}_l/\mathrm{d}y|. \quad [10]$$

Figure 14 represents a comparison between the mixing lengths obtained in the above mentioned ways. A satisfactory agreement can be seen between them within the range $-0.85 < r/R < -0.25$. Values of the mixing length for momentum transport deduced from [8] are given in figure 15 together with a mixing length correlation for single-phase flow (broken line) given by

$$L_m/R = 0.14 - 0.08(r/R)^2 - 0.06(r/R)^4. \quad [11]$$

This figure indicates much larger values of the mixing length in bubbly flow than in single-phase water flow. From this we may realize that the turbulent transport is more active in bubbly flow than in single-phase flow, which coincides completely with the experimental indications of the flattened distributions of water velocity and phases. It is apparent that the mixing length is a strong function of the void fraction and possibly of the water velocity. The results show that as the void fraction or the quality increases, the mixing length first increases rapidly up to a certain value determined mainly by water velocity, and finally decreases towards the value for single-phase flow. These values are greatly different from those obtained by Brandt (1958).

According to the mixing length theory, the eddy diffusivity for momentum transport ϵ_M is

†According to Malnes (1966), the term $\bar{V}_l\overline{\rho' v}$ should be zero. However, details are to be known about such an argument. We will not discuss its validity here.

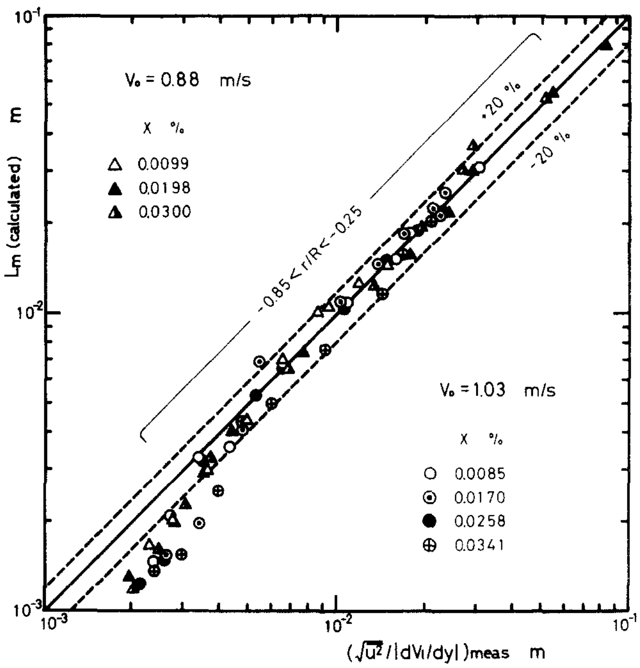

Figure 14. Correlative representation between mixing lengths calculated in two ways.

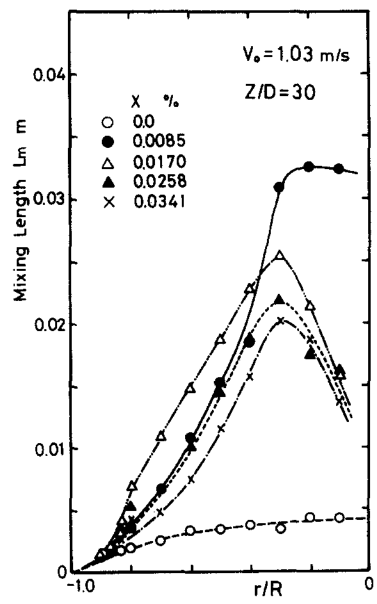

Figure 15. Mixing length for momentum transport.

defined by

$$\epsilon_M = L_m^2(\mathrm{d}\bar{V}_l/\mathrm{d}y). \qquad [12]$$

Typical results obtained are illustrated in figure 16. It is noted that the diffusivities are not affected very greatly by a change in gas flow rate, and that they pass through a maximum at a point intermediate between the wall and the pipe center ($r/R \simeq -0.3$).

Here, it is of great interest to consider the momentum transport rates caused by three contributing terms. Let Γ_v, Γ_d, and Γ_{vs} the momentum transport rates due to the velocity

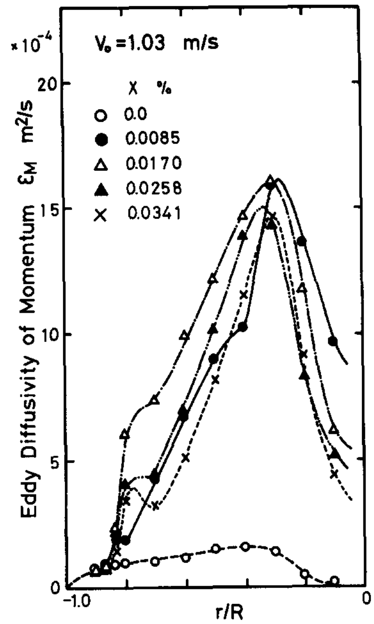

Figure 16. Eddy diffusivity for momentum transport.

fluctuation, the density fluctuation, and the viscous force, respectively. Then we have

$$\Gamma_v = \rho_l L_m{}^2 \bar{\alpha}_l |d\bar{V}_l/dy|(d\bar{V}_l/dy),$$

$$\Gamma_d = \rho_l L_m{}^2 |d(\bar{\alpha}_l \bar{V}_l)/dy|(d\bar{V}_l/dy), \qquad [13]$$

$$\Gamma_{vs} = \mu_l \bar{\alpha}_l (d\bar{V}_l/dy).$$

Results are shown in figure 17 where Γ_v/Γ_{vs} and Γ_d/Γ_{vs} are plotted as a function of radius. As expected, it is seen that both contributions due to the turbulent fluid motions (Γ_v and Γ_d) are thus two or three orders of magnitude greater than the viscous effect. It is noted that the turbulent

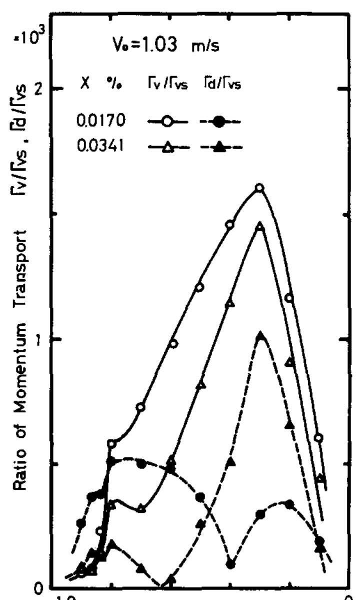

Figure 17. Momentum transport ratios.

velocity contribution Γ_v is higher than the density contribution Γ_d for the range of variables tested within the range $|r/R| < 0.8$, and in the outer region the latter is dominant. This observation means that in case of low void fraction, momentum transport will be carried out mainly by the turbulent velocities of the liquid phase, except in the wall proximity region. Towards the wall region, to which bubbles are apt to gather as seen in figure 6 in the previous paper of this series, it is carried out by density fluctuation due to the violent stirring effect of bubbles, or due to the wall effect.

CONCLUSIONS

Turbulent transport of heat and bubbles has been studied in the core region of air–water two-phase bubbly flow in a pipe, and also in water flow. Data reduction of the helium concentration (or bubble impaction rate) and temperature distributions were carried out to determine the turbulent bubble dispersion coefficient ϕ and the eddy diffusivity for heat transport ϵ_H. Finally, the momentum transport was discussed according to the mixing length concept. The following main conclusions may be presented:

(1) The turbulent velocity components of the liquid phase play a predominant role in the turbulent transport process of heat, momentum, and bubbles in common.

(2) A systematic increase of the diffusivity ϵ_H with the quality and the water velocity was observed.

(3) The diffusivity ratio $\epsilon_{H,TP}/\epsilon_{H,SP}$ correlates with the Martinelli modulus X_{tt} by the following empirical equation,

$$\epsilon_{H,TP}/\epsilon_{H,SP} = 1 + 462 X_{tt}^{-1.27}.$$

(4) A bubble diffusion model appears to be applicable for describing the turbulent transport of bubbles in single-phase water flow and also in air–water two-phase bubbly flow within the core region of the flow area where local flow variables are uniformly distributed. The bubble dispersion coefficient can be well defined there.

(5) No systematic variation of bubble dispersion coefficient ϕ with the water velocity was observed, while ϕ increases with increasing quality.

(6) The Péclet number $u_c'\bar{d}/\phi$ can be approximated by 2.0 independent of quality and water velocity.

(7) The diffusivity ratio ϕ/ϵ_H decreases to unity dependent upon the quality and the water velocity. A smaller value of ϕ/ϵ_H is related to a higher water velocity for constant quality.

(8) It may be evaluated from a mixing length concept that the dominant mechanism of the turbulent transport process in air–water bubbly flow is subjected to the turbulent velocity components of the liquid phase, and the contribution due to the density fluctuation is an additional term.

Acknowledgements—The authors express their gratitude to Mr. T. Zigami for his aid in the operation of the experiments.

REFERENCES

AOKI, S., INOUE, A. & YAEGASHI, H. 1969 The local void fraction and velocities of the phases in two-phase bubbly flow in a vertical tube. *Proc. 6th Japan. Heat Transfer Symp.* pp. 241–244.

BRANDT, F. 1958 Der reibungsdruckverlust von wasser-dampf-gemischen und die voreilgeschwindigkeit des dampfes gegenüber dem wasser in senkrechten kesselrohren. Dissertation, Darmstadt.

BRILLER, R. & ROBINSON, M. 1969 A method for measuring particle diffusivity in two-phase flow in the core of a duct, *A.I.Ch.E. Jl* **15**, 733–735.

COUSINS, L. B. & HEWITT, G. F. 1968 Liquid Phase Mass Transfer in Annular Two-Phase Flow: Radial Liquid Mixing. *AERE-R* 5693.

GINSBERG, T. 1971 Droplet Transport in Turbulent Pipe Flow. *ANL*—7694.

GOLDSCHMIDT, V. M., HOUSEHOLDER, M. K., AHMADI, G. & CHUANG, S. C. 1972 Turbulent diffusion on small particles suspended in turbulent jets. *Progr. Heat Mass Transfer* **6**, (Edited by HETSRONI, G., SIDEMAN, S. & HARTNETT, J. P.). pp. 487–508, Pergamon.

HINO, M. 1967 Micro-structure of solid–liquid two-phase flow. *Proc. Symp. on Multi-Phase Mixture.* pp. 21–30. Prepared by Sci. Council of Japan.

HINZE, J. O. 1959 *Turbulence*, McGraw-Hill.

HOUGHTON, G. 1961 Some theoretical aspects of vapor void formation in heated vertical channels, *Nucl. Sci. Engng* **11**, 121–128.

HOUGHTON, G. 1962 An analysis of vapor void profiles in heated channels, *Nucl. Sci. Engng* **12**, 390–397.

LEVY, S. 1963 Prediction of two-phase pressure drop and density distribution from mixing length theory, *Trans. Am. Soc. Mech. Engrs Ser. C* **85**, 137–152.

MALNES, D. 1966 Slip Ratios and Friction Factors in the Bubble Flow Regime in Vertical Tubes. *KR*—110.

OKAMOTO, Y., HANAWA, H. & KAMEOKA, T. 1971 A study of channel flow using hydrogen bubble tracer technique, *Trans. Japan Soc. Mech. Engrs* **37**, 305–312.

REITH, T., RENKEN, S. & ISRAEL, B. A. 1968 Gas hold-up and axial mixing in the fluid phase of bubble columns. *Chem. Engng Sci.* **23**, 619–629.

SERIZAWA, A., KATAOKA, I. & MICHIYOSHI, I. 1973 Turbulence structure of air–water bubbly flow (III). *Proc.* 1973 *Fall Meet. At. Energy Soc. Japan*, B3.

SERIZAWA, A. 1974 Fluid-Dynamic Characteristics of Two-Phase Flow. Doctoral Thesis, Kyoto University.

SUNEJA, S. K. & WASAN, D. T. 1972 Dispersion of charged particles in a turbulent air stream under transverse flow conditions, *Ind. Engng Chem. Fundam.* **11**, 57–66.

Auszug—Eine experimentelle Studie von Waerme- und Blasentransport in turbulenter Luftblasen-Wasserstroemung wurde mit Hilfe einer Tracertechnik durchgefuehrt. Auf Grund von Angaben ueber Helium-Tracergaskonzentration und Temperaturverteilung wurde die Diffusivitaet von Blasen und Waerme bestimmt. Die Ergebnisse weisen auf die entscheidende Rolle hin, die die turbulenten Geschwindigkeitskomponenten der Fluessigkeitsphase beim turbulenten Transportprozess spielen. Ein systematisches Ansteigen der Waermediffusivitaet ϵ_H mit Luftanteil und Wassergeschwindigkeit war zu beobachten. Eine empirische Korrelation fuer das Diffusivitaetsverhaeltnis $\epsilon_{H,TP}/\epsilon_{H,SP}$ wird angegeben. Die Pécletsche Zahl $u'_c\bar{d}/\phi$ der Blasendispersion kann annaehernd, unabhaengig von den Stroemungsparametern, gleich 2·0 gesetzt werden. Das Verhaeltnis von Blasen- zu Waermediffusivitaet ϕ/ϵ_H naehert sich mit Ansteigen des Luftanteils und der Wassergeschwindigkeit dem Wert 1. Der Bewegungsgroessentransport wird auf Grund der Mischungswegstheorie eroertert.

Резтоме—Эксперименальное исследование переноса тепла и пузырьков в турбулентном водо-воздушном пузырьковом течение было выполнено посредством меченных атомов. Сведения о концентрации меченного гелия были использованы для получения информации о рассеянии пузырьков и тепла. Результаты показывают, что составляющие турбулентной скорости жидкой фазы играют первостепенную роль в процессе турбулентного переноса. Было наблюдено постоянное повышение рассеиваемости тепла ε_H при повышении качества и скорости воды. Приведено эмпирическое соотношение для отношения рассеиваемосте $\varepsilon_{H,TP}/\varepsilon_{H,SP}$. Критерний Пекле $\varepsilon]c\alpha/\phi$ для пузырькового рассеяния может быть представлен приближенно как 2,0 вне зависимости от переменных, описысывающих течение. Отношение рассеиваемостей пузырьков и тепла ϕ/ε_H достигает половины единицы при повышении качества и скорости воды. Транспортирующий момент количества движения обсуждается аналогично, что основано на теории смешиваемой длины.